Environmental Pollution 235 (2018) 534–545

Contents lists available at ScienceDirect

Environmental Pollution

journal homepage: www.elsevier.com/locate/envpol

Investigation of silver (Ag) deposition in tissues from stranded cetaceans by autometallography (AMG)☆

Wen-Ta Li [a], Hui-Wen Chang [a], Meng-Hsien Chen [b], Hue-Ying Chiou [c], Bang-Yeh Liou [a], Victor Fei Pang [a], Wei-Cheng Yang [d, **], Chian-Ren Jeng [a, *]

[a] Graduate Institute of Molecular and Comparative Pathobiology, National Taiwan University, Taipei, Taiwan, ROC
[b] Department of Oceanography and Asia-Pacific Ocean Research Center, National Sun Yat-sen University, Kaohsiung, Taiwan, ROC
[c] Graduate Institute of Veterinary Pathobiology, National Chung Hsing University, Taichung, Taiwan, ROC
[d] College of Veterinary Medicine, National Chiayi University, Chiayi, Taiwan, ROC

ARTICLE INFO

Article history:
Received 28 October 2017
Received in revised form
2 January 2018
Accepted 4 January 2018

Keywords:
Autometallography
Cetacean
Inductively coupled plasma mass spectrometry (ICP-MS)
Silver (Ag)

ABSTRACT

Silver, such as silver nanoparticles (AgNPs), has been widely used in commercial products and may be released into the environment. The interaction between Ag deposition and biological systems is raising serious concerns because of one health consideration. Cetaceans, as the top predators of the oceans, may be exposed to Ag/Ag compounds and suffer negative health impacts from the deposition of these compounds in their bodies. In the present study, we utilized autometallography (AMG) to localize the Ag in the liver and kidney tissues of cetaceans and developed a model called the cetacean histological Ag assay (CHAA) to estimate the Ag concentrations in the liver and kidney tissues of cetaceans. Our results revealed that Ag was mainly located in hepatocytes, Kupffer cells and the epithelial cells of some proximal renal tubules. The tissue pattern of Ag/Ag compounds deposition in cetaceans was different from those in previous studies conducted on laboratory rats. This difference may suggest that cetaceans have a different metabolic profile of Ag, so a presumptive metabolic pathway of Ag in cetaceans is advanced. Furthermore, our results suggest that the Ag contamination in cetaceans living in the Northwestern Pacific Ocean is more severe than that in cetaceans living in other marine regions of the world. The level of Ag deposition in cetaceans living in the former area may have caused negative impacts on their health condition. Further investigations are warranted to study the systemic Ag distribution, the cause of death/stranding, and the infectious diseases in stranded cetaceans with different Ag concentrations for comprehensively evaluating the negative health effects caused by Ag in cetaceans.

1. Introduction

Commercial products containing silver (Ag) have been used for over 100 years, and awareness of Ag contamination in the environment has markedly increased due to the extensive use of silver nanoparticles (AgNPs) (Nowack et al., 2011). AgNPs have been used in numerous commercial products, such as water filters, textiles, cosmetics, food packaging and medical items, mainly due to their strong antimicrobial properties (Yu et al., 2013). AgNPs also have unique physicochemical properties, such as high electrical and thermal conductivities, so they are increasingly applied in electronic devices and medical imaging (Ajmal et al., 2016; Ge et al., 2014). The production of AgNPs and the number of AgNP-containing products has dramatically increased in the last decade and is expected to increase over time (Hansen et al., 2016; Vance et al., 2015). AgNPs can be released during the production, transport, erosion, washing, and/or disposal of AgNP-containing products, subsequently draining into the aquatic environment and ultimately accumulating in the ocean (Farre et al., 2009; Walters et al., 2014). The fate of AgNPs in the aquatic environment is complicated and variable. Previous studies indicated that AgNPs in the aquatic environment can remain as individual particles in suspension, aggregate, dissolve, react with different species in the environment, or be regenerated from silver ions (Levard et al., 2012; Massarsky et al., 2014). Furthermore, different types of Ag speciation, such as AgCl, Ag_2S, and Ag_0, can be found in marine

☆ This paper has been recommended for acceptance by Maria Cristina Fossi.
* Corresponding author.
** Corresponding author.
E-mail addresses: jackywc@gmail.com (W.-C. Yang), crjeng@ntu.edu.tw (C.-R. Jeng).

https://doi.org/10.1016/j.envpol.2018.01.010
0269-7491/

sediments contaminated with AgNPs, where they are ingested by benthic organisms and subsequently enter the food chain in marine environments (Wang et al., 2014). The increasing use and growing production of AgNPs, as potential sources of Ag contamination, raise public concern about the environmental toxicity of Ag.

Ag can be transferred from one trophic level to the next via the food chain and may cause negative effects on the animals at higher trophic levels, such as cetaceans (Buffet et al., 2014; Farre et al., 2009; Wang et al., 2014), and cetaceans have been thought to suffer potentially detrimental impacts from excessive silver exposure (Chen et al., 2017). The Ag concentrations in cetaceans have been investigated by several studies in different countries, and their results have varied among different organs, age classes, animal species, and habitats (Dehn et al., 2006; Reed et al., 2015; Romero et al., 2017; Seixas et al., 2009). The levels of unhealthy and critically dangerous concentrations of Ag in small cetaceans of the North Pacific Ocean have been established, and the suggested threshold concentrations of Ag are 0.43 ± 0.28 and 0.08 ± 0.03 μg/g dry weight for liver and kidney tissues, respectively (Chen et al., 2017). A recent study conducted in Taiwan found an extremely high Ag concentration (726.11 μg/g dry weight) in the liver tissue of a stranded Fraser's dolphin (*Lagenodelphis hosei*), which implies that dolphins in the marine environment of the North-western Pacific Ocean may have severe Ag contamination (Chen et al., 2017). Cetaceans are longevous, and being at the highest trophic levels of marine ecosystem, and they share common food resources with humans. The bioaccumulation effect of anthropogenic contaminants in cetaceans may eventually occur in humans (Bossart, 2011). These reasons further support that cetaceans are ideal sentinel animals for evaluating the health of marine environments and humans. Hence, it is crucial to determine the contamination status (e.g., tissue concentrations and distribution) of Ag in cetaceans.

Generally, the concentrations of trace metals in cetacean tissues are determined by inductively coupled plasma mass spectroscopy (ICP-MS) (Caceres-Saez et al., 2013; Chen et al., 2017; Mendez-Fernandez et al., 2014; Romero et al., 2017). The advantages of using ICP-MS include the provision of quantitative data with favourable detection limits (0.01–0.1 μg/L), simple specimen preparation, and the capability of simultaneous measurement of several elements (Nuttall et al., 1995). However, ICP-MS still has some disadvantages. The capital cost for establishing the ICP-MS and sample storage (including instruments, electricity charges and consumables) are relatively high (Bornhorst et al., 2005; Nuttall et al., 1995). In addition, ICP-MS detects target contaminants only on the organ level, and not the histological location or cell level (Miller et al., 2016). The standard procedure of tissue samples collection from stranded cetacean for ICP-MS analysis usually requires a relatively large sized frozen tissue sample ($6 \times 6 \times 6$ cm, approximately 200 g) due to the possibility of contamination during sample collection in the field environment (Geraci and Lounsbury, 2005), and these frozen samples may not be easy to store in limited refrigeration space. Furthermore, complete sample collection from the stranded cetaceans were seriously limited by several factors including difficulties of logistics and shortage of manpower. Therefore, the samples can be collected are usually the formalin fixed samples. If a relatively rapid, easy to use and inexpensive methodology by using the formalin fixed samples is developed, it will facilitate investigation of the suborgan distribution and concentration of target contaminants in cetaceans.

Formalin-fixed, paraffin-embedded (FFPE) tissues can be a sample resource for molecular analysis (such as polymerase chain reaction) and metal measurements (Bischoff et al., 2008; Bonta et al., 2017; Kokkat et al., 2013; Tran et al., 2014). Bonta et al. (2017) found that the FFPE process caused severe alteration in the suborgan distributions and concentrations of alkali and alkaline earth metals but led to lesser effects on those of transition metals. In addition, previous studies have indicated that heavy metals can be amplified in FFPE tissue sections by autometallography (AMG), which is a histochemical process, and thereby can be visualized under light microscopy (Anderson et al., 2015; Danscher, 1991; Kim et al., 2009; Miller et al., 2016). Although the AMG method may have a relatively low sensitivity (comparing to ICP-MS), difficulty to unveil a homogenously diffused material, underestimation of the content in case of a great concentration of heavy metals in a narrowed surface, it is still a valuable method to study the suborgan distribution of heavy metals. Furthermore, AMG method may amplified a group of trace metals, including gold, silver, mercury, bismuth and zinc, and thus the results of AMG method may be interfered by other trace metals (Stoltenberg and Danscher, 2000). Therefore, the interpretation of AMG positivity signals in the tissue from wild animals (which are not an intentional and well-controlled exposure to a single product) should be incorporated with other specific methods to monitor the actual composition of heavy metals, such as ICP-MS (Stoltenberg and Danscher, 2000). The quantitative analysis of histological tissue sections with histochemical staining has been developed by the use of digital image analysis software, such as imageJ (Deroulers et al., 2013; Jensen, 2013; Parlee et al., 2014; Shu et al., 2016). The present study utilized the histochemical technique (autometallography; AMG) to localize Ag in cetacean tissues, investigated the histopathological lesions possibly caused by the Ag, and developed an assay to estimate the Ag concentration in the liver and kidney tissues of cetaceans by a regression model based on the data from image quantitative analysis and ICP-MS.

2. Materials and methods

2.1. Sample source

The research permit (104-07.1-SB-62) for the cetacean sample collection was provided by Council of Agriculture of Taiwan. From 1999 to 2016, liver and kidney tissues from 110 stranded cetaceans of 7 different species, including 22 *Feresa attenuata* (Fa), 5 *Grampus griseus* (Gg), 38 *Kogia* spp. (Ko), 13 *Lagenodelphis hosei* (Lh), 13 *Stenella attenuata* (Sa), 8 *Steno bredanensis* (Sb), and 11 *Tursiops truncatus* (Tt), were collected. A field number was given to each cetacean for individual identification. The liver and kidney tissues used in the present study were from freshly dead and moderately autolysed stranded cetaceans (Geraci and Lounsbury, 2005). Some liver and kidney tissues were collected from live stranded cetaceans after they died during rescue or rehabilitation efforts. Each individual was classified into 1 of 2 age classes (young or adult) by relative measures of age, such as body length, tooth wear, the presence of hair follicles on rostrum and lingual marginal papillae, skin colour, the status of reproductive organs, and/or fusion of cranial sutures (Hohn, 2009), since age determination by the growth layers of teeth was not done in all individuals. The biological characteristics of each cetacean species are summarized in Table 1.

In total, 220 formalin fixed tissue samples (110 from liver and 110 from kidney) were collected for subsequent histological analysis. Among these 110 stranded cetaceans, only 12 frozen tissue samples (6 from liver and 6 from kidney) were collected, put into zip-lock plastic bags, and stored at −20 °C for determination of Ag concentrations by ICP-MS.

2.2. AMG reactivity of formalin-fixed tissues

The representative formalin-fixed tissues of liver and kidney

Table 1
Biological characteristics and estimated Ag concentrations (mean ± SD, μg/g) in the liver and kidney tissues of *Feresa attenuata, Grampus griseus, Kogia spp., Lagenodelphis hosei, Stenella attenuata,* and *Steno bredanensis, Tursiops truncatus* from Taiwan. N: sample size; U: unknown sex.

	All species					*Feresa attenuata*					*Grampus griseus*					*Kogia* spp.				
	N	Liver		Kidney		N	Liver		Kidney		N	Liver		Kidney		N	Liver		Kidney	
		Mean	SD	Mean	SD		Mean	SD	Mean	SD		Mean	SD	Mean	SD		Mean	SD	Mean	SD
All	110	10.49	6.48	0.50	0.45	22	12.95	6.64	0.91	0.43	5	12.67	7.09	0.43	0.36	38	9.32	6.08	0.38	0.36
Adult	84	12.82	5.32	0.63	0.43	19	14.74	5.17	1.04	0.28	4	15.14	5.13	0.54	0.32	28	11.61	5.36	0.49	0.35
Young	26	2.97	3.42	0.08	0.10	3	1.68	1.51	0.07	0.06	1	2.79	–	0.02	–	10	2.92	1.96	0.08	0.14
Female	36	9.55	5.69	0.58	0.51	8	12.43	6.05	0.96	0.43	1	12.03	–	0.35	–	12	8.53	6.04	0.50	0.52
Male	59	10.88	7.05	0.41	0.38	7	11.94	8.82	0.76	0.55	3	11.64	9.58	0.27	0.22	25	9.74	6.30	0.32	0.25
U	15	11.24	6.03	0.70	0.48	7	14.56	5.42	0.99	0.29	1	16.37	–	1.01	–	1	8.43		0.54	
	Lagenodelphis hosei					*Stenella attenuata*					*Steno bredanensis*					*Tursiops truncatus*				
	N	Liver		Kidney		N	Liver		Kidney		N	Liver		Kidney		N	Liver		Kidney	
		Mean	SD	Mean	SD		Mean	SD	Mean	SD		Mean	SD	Mean	SD		Mean	SD	Mean	SD
All	13	6.96	6.87	0.44	0.46	13	12.65	6.28	0.63	0.44	8	11.89	6.13	0.14	0.13	11	9.27	5.60	0.33	0.42
Adult	6	13.43	4.32	0.85	0.35	10	13.62	6.15	0.77	0.40	7	13.42	4.67	0.16	0.12	10	10.11	5.11	0.36	0.43
Young	7	1.41	0.99	0.08	0.07	3	9.43	6.76	0.18	0.06	1	1.15	–	0.01	–	1	0.83	–	0.01	–
Male	4	8.69	5.51	0.56	0.42	3	5.85	3.59	0.67	0.46	4	9.57	6.45	0.09	0.08	4	9.86	5.85	0.53	0.69
Female	8	6.75	7.88	0.42	0.52	8	15.51	5.83	0.58	0.42	4	14.21	5.64	0.19	0.15	4	11.29	6.28	0.28	0.07
U	1	1.66	–	0.09	–	2	11.43	1.08	0.78	0.76	0	–	–	–	–	3	5.77	4.36	0.12	0.10

from each individual were selected (random or the regions with significant lesions), trimmed, dehydrated through a series of graded ethanol, and then infiltrated with paraffin. The FFPE tissues were sectioned at 5 μm, deparaffinised with xylene, treated with 0.5% Triton X-100 in phosphate-buffered saline (PBS), and washed several times with PBS and double-distilled water. The tissue sections were stained by silver enhancement method (Kim et al., 2009; Miller et al., 2016) and counterstained with hematoxylin for 10 s. The tissue sections were air dried, mounted with Canada balsam, and examined under a light microscope (Nikon ECLIPSE Ni-U, Nikon Corporation, Japan). The AMG positive signals were golden yellow to black dots or amorphous golden yellow substances. Images were captured using a Nikon ECLIPSE Ni-U microscope connected to a digital camera (Nikon DS-Fi2, Nikon Corporation) and computer imaging software (NIS-Elements D, Nikon Corporation). Ten histological images were randomly captured with a 40X objective lens from each tissue section and used in semi-quantitative analysis.

2.3. Semi-quantitative analysis for AMG positivity of histological images

Semi-quantitative analysis on these histological images was performed using ImageJ (National Institutes of Health, Bethesda, MD). Briefly, the histological images were split into three colour channels (red, blue, and green), and the blue channel was used for quantifying the AMG positive signals. The cut-off values of the threshold levels for each histological image were manually adjusted (from 90 to 110) due to the presence of false positive areas in nuclei and/or red blood cells, and the positive percent area of each histological image was displayed in the “Result” window. The positive percent areas of 10 histological images from each tissue section were averaged and defined as the AMG positivity value for each tissue section. However, the distribution pattern of the AMG positive signals (such as high concentration of AMG positive signals in a single region rather than a homogenous ground of AMG positive signals in the whole section) may affect the results of semi-quantitative analysis, the reliability of the semi-quantitative analysis should be seriously evaluated with the pattern of the AMG positive signals.

2.4. The correlation between the results of ICP-MS and AMG positivity values

The Ag concentrations of the liver and kidney tissues were determined using ICP-MS according to previously published methods (Chen et al., 2002, 2017). In total, 6 liver and 6 kidney tissues from 6 cetaceans, including 2 Ko, 1 Gg, 2 Lh, and 1 Sa, were investigated. Data from the liver and kidney tissues were analysed separately. The strength of association between the results of ICP-MS and AMG positivity values from the same liver and kidney tissues were analysed by Pearson correlation analysis.

2.5. Establishment of the Cetacean Histological Ag Assay (CHAA)

The Ag concentrations of the liver and kidney tissues with unknown Ag concentrations were estimated by regression models based on AMG positivity values from cetacean tissues with known Ag concentration, hereafter referred to as the Cetacean Histological Ag Assay (CHAA) for livers and kidneys. The flowchart of the strategy to estimate the concentration of Ag by AMG through CHAA was illustrated (Fig. 1). The regression models were compared using the extra sum-of-squares F test and Akaike's information criterion (AIC) (Liang et al., 2017; Spiess and Neumeyer, 2010). Most importantly, the selected model had to generate scientifically valid results. For instance, if one of the regression models estimated unrealistic Ag concentrations, the regression model was abandoned. The effect size for the selected regression model was reported by adjusted R^2.

The accuracy of the CHAA for livers and kidneys was evaluated by the mean standard deviation (SD) calculated from differences between known and estimated Ag concentrations (Polanowski et al., 2014). The precision of the semi-quantitative analysis by ImageJ in the liver and kidney tissues of cetaceans was evaluated by repeated measurement of AMG positivity values of serial sections from the same FFPE tissues. Three liver and 3 kidney tissues with known Ag concentrations of 0.06, 14.93, 21.82, 0.05, 1.04 and 0.42 μg/g were analysed 3 times each. The mean SDs for 9 measurements from liver and kidney tissues were calculated from differences between known and estimated Ag concentrations and used to evaluate the precision of the semi-quantitative analysis for AMG positivity (Polanowski et al., 2014).

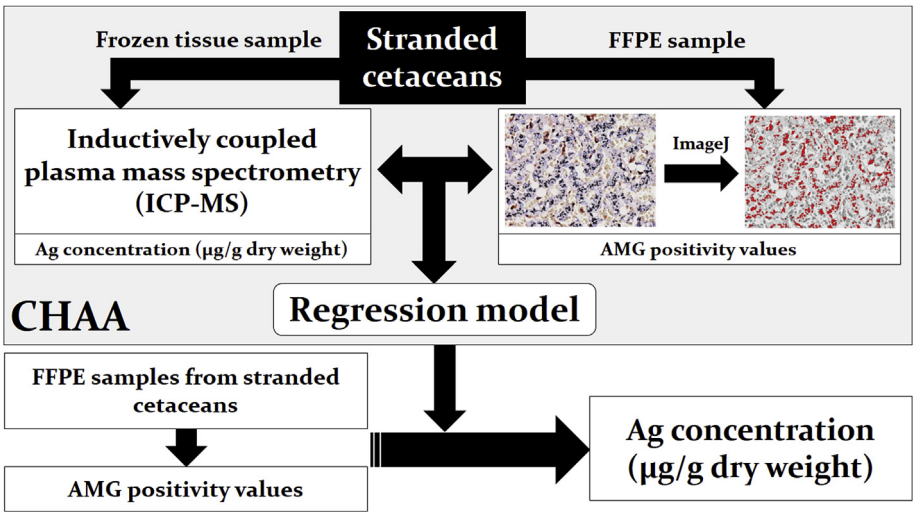

Fig. 1. Flowchart of the strategy to estimate the concentration of Ag by autometallography (AMG) through cetacean histological Ag assay (CHAA).

2.6. Estimation of Ag concentrations in FFPE tissue sections

The Ag concentrations of the liver and kidney tissues of cetaceans not investigated by ICP-MS were estimated by CHAA. The estimated Ag concentrations of liver and kidney tissues were first checked by D'Agostino-Pearson normality test, and the data were not normally distributed. Therefore, the Kruskal-Wallis Test (post hoc test: Dunn's multiple comparison test) and Mann-Whitney *U* test were used for further analysis. Three parameters—age class, sexuality, and species—were analysed. All data were plotted on box-plot graphics. The bar in the middle of the box represented the second quartile (median), and the bottom and top of the box described the first and third quartiles. The whiskers showed the 75th percentile plus 1.5 times IQR and 25th percentile minus 1.5 times IQR of all data, and any values greater than these were defined as outliers and plotted as individual points. Different letters above the boxplots indicated statistically significant differences ($p < .05$) between groups. The baseline and unhealthy Ag concentrations in the liver tissue were defined as 0.43 μg/g and 4.45 μg/g, respectively; the baseline and unhealthy Ag concentrations in the kidney tissues were defined as 0.08 μg/g and 0.33 μg/g, respectively (Chen et al., 2017).

2.7. Histopathological findings in liver and kidney tissues with different estimated silver concentrations

The FFPE samples were sectioned at 5 μm and stained with hematoxylin and eosin (H&E) for histopathological examination. The slides were comprehensively examined in a blinded fashion by a single veterinary pathologist (Wen-Ta Li), and the lesions in liver and kidney were recorded and categorized. The direct correlation between the lesions and Ag was evaluated by the intralesional aggregates of AMG positive signals. The correlation between the lesions (presented or unpresented) and estimated Ag concentrations were analysed by Chi-square test or Fisher exact test. The liver tissues with estimated Ag concentrations ≤0.43, 0.43–4.45, and ≥4.45 μg/g were respectively classified into baseline, intermediate, and unhealthy groups; the kidney tissues with estimated Ag concentrations ≤0.08, 0.08–0.33, and ≥0.33 μg/g were respectively classified into baseline, intermediate, and unhealthy groups.

3. Results

3.1. Patterns of AMG positive signals in the liver and kidney tissues

Different patterns of AMG positive signals were detected in the liver and kidney tissues of cetaceans. Because the AMG positive signals may be interfered by other heavy metals, the liver and kidney tissues with Ag concentrations higher than baselines measured by ICP-MS were used as the positive group to demonstrate the Ag distribution. In the livers of positive group (5 individuals, Table 2), the AMG positive signals were diffusely/evenly distributed in hepatic parenchyma and were variably sized brown to black dots in hepatocytes and Kupffer cells (Fig. 2A and B). In the kidneys of positive group (3 individuals, Table 2), the AMG positive signals were variably-sized brown to black dots and unevenly distributed in the epithelial cells of some proximal renal tubules in the renal cortex (Fig. 2C and D). Golden-yellow to brown AMG positive signals in the basement membranes of renal tubules and glomeruli and amorphous golden-yellow to brown AMG positive signals on the surface of epithelial cells of proximal renal tubules were found in one individual *(Lagenodelphis hosei*; field code: TP20110830) (Fig. 2E). In contrast, absent to minimal AMG positive signals (the majority being brown to black dots) were noted in the livers (Fig. 2F) and kidneys (Fig. 2G) of individuals with Ag concentrations lower than baselines (Table 2).

Table 2
The results of ICP-MS and AMG positivity values from six cetaceans. Gg = *Grampus griseus*, Ko = *Kogia* spp., Lh = *Lagenodelphis hosei*, Sa = *Stenella attenuata*, M = Male, F = Female, AMG = AMG positivity values quantified by imageJ, ICP-MS = Ag concentrations measured by ICP-MS (μg/g, dry weight).

Field number	Species	Sex	Age class	Liver		Kidney	
				AMG	ICP-MS	AMG	ICP-MS
TP20111116	Gg	M	Adult	7.48	21.82	8.82	0.42
TC20110611	Ko	M	Adult	4.50	2.77	1.52	0.05
TC20110722	Ko	M	Young	1.20	3.86	0.11	0.05
TD20110608	Lh	M	Young	0.34	0.06	0.21	0.05
TP20110830	Lh	M	Adult	6.21	14.93	9.43	1.04
IL20110101	Sa	F	Young	2.67	1.73	5.26	0.14

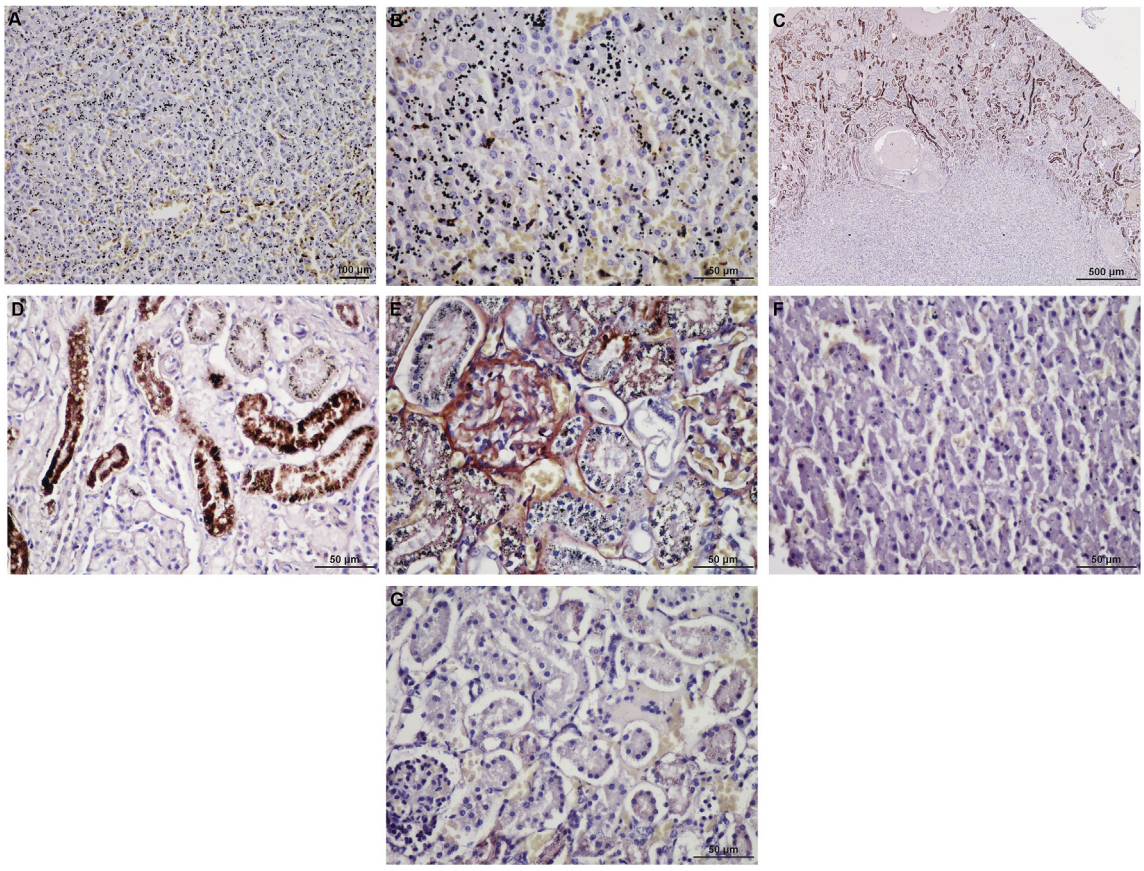

Fig. 2. Representative photographs of the Autometallography (AMG) positive signals in the liver and kidney tissues of cetacean. Silver enhancement method with hematoxylin as counterstain. (A) The AMG positive signals in the liver with a higher Ag concentration (14.93 μg/g) are diffusely and evenly distributed in the hepatic parenchyma (*Lagenodelphis hosei* (Lh); field code: TP20110830). (B) Higher magnification of Fig. 1A. The AMG positive signals are variably sized brown to black dots in hepatocytes and Kupffer cells. (C) The AMG positive signals in the kidney with a higher Ag concentration (1.04 μg/g) are unevenly distributed in the renal cortex (Lh; field code: TP20110830). (D) Higher magnification of Fig. 1C. The AMG positive signals are variably sized brown to black dots in the epithelial cells of proximal renal tubules. (E) Golden-yellow to brown AMG positive signals on the basement membranes of renal tubules and glomeruli and amorphous golden-yellow to brown AMG positive signals on the surface of epithelial cells of proximal renal tubules are occasionally found in the kidney tissue of one individual (Lh; field code: TP20110830). (F) Scattered AMG positive signals of brown to black dots are observed in the liver with a lower Ag concentration (0.06 μg/g) (Lh; field code: TD20110608) (G) Scattered AMG positive signals of brown to black dots are observed in the liver with a lower Ag concentration (0.05 μg/g) (Lh; field code: TD20110608). (For interpretation of the references to colour in this figure legend, the reader is referred to the Web version of this article.)

3.2. Establishment of the Cetacean Histological Ag Assay (CHAA)

The results of ICP-MS and AMG positivity values in the six stranded cetaceans are summarized in Table 2. Significant positive correlations between the results of ICP-MS and AMG positivity values were found in the liver (Pearson's $r = 0.88$; $p = .0204$) and kidney (Pearson's $r = 0.83$; $p = .0393$) tissues. The regression models to establish the CHAA for livers and kidneys, including linear regression, quadratic regression, cubic regression and linear regression through origin, were statistically compared, and linear regression through origin was the preferred regression model for the CHAA (Table 3). The regression equations of the CHAA for livers and kidneys were respectively $Y = 2.249 \times X$ (adjusted $R^2 = 0.74$) and $Y = 0.07288 \times X$ (adjusted $R^2 = 0.69$) (Fig. 3A and B). The mean standard deviations from six FFPE tissue sections with known Ag concentrations to evaluate the accuracy of the CHAA were 3.24 and 0.16 for livers and kidneys, respectively. In addition, the mean standard deviations of three repeated measurements of the same FFPE tissue sections with known Ag concentrations to evaluate the consistency of CHAA were 2.8 and 0.35 for livers and kidneys, respectively.

3.3. Estimation of Ag concentrations of the liver and kidney tissues by CHAA

The estimated Ag concentrations presented as mean ± SD of each cetacean species are summarized in Table 1. The ranges of estimated Ag concentrations were 0.06–28.39 and 0–1.6 μg/g in the liver and kidney tissues, respectively. There was a significant age-dependent increase of Ag concentration in the liver (12.82 ± 5.3 and 3.0 ± 3.4 μg/g) and kidney (0.63 ± 0.43 and 0.08 ± 0.10 μg/g) tissues (Fig. 4A), and the Ag concentrations of liver tissues (10.49 ± 6.48 μg/g) were significantly higher than those of kidney tissues (0.50 ± 0.45 μg/g) (Fig. 4B). No significant difference in Ag concentrations between sexes in the liver and kidney tissues was observed (Fig. 4C), nor was a significant difference in Ag concentrations in the liver tissues found among these cetacean species. In approximately 50% of the individuals, the estimated Ag concentrations of the liver tissues were higher than the unhealthy Ag concentration (Fig. 4D). The Ag concentrations in the kidney tissues of Fa (0.93 ± 0.45 μg/g) were significant higher than those of Ko (0.38 ± 0.37 μg/g), Tt (0.32 ± 0.45 μg/g) and Sb (0.12 ± 0.13 μg/g). In approximately 30% of the individuals, the estimated Ag

Table 3
The comparisons among different regression models to establish the Cetacean Histology Ag Assay (CHAA) for liver and kidney tissues of cetaceans by the extra sum-of-squares F test and Akaike's information criterion (AIC).

	Extra sum-of-squares F test					
	CHAA for liver			CHAA for kidney		
Null hypothesis	Linear regression through origin			Linear regression through origin		
Alternative hypothesis	Linear	Quadratic	Cubic	Linear	Quadratic	Cubic
P value	0.4644	0.1065	0.2621	0.8201	0.354	0.4559
Conclusion (α = 0.05)	Not reject	Not reject	Not reject	Not reject	Not reject	Not reject
Preferred model	Linear regression through origin			Linear regression through origin		
F (DFn, DFd)	0.6529 (1,4)	5.174 (2,3)	2.969 (3,2)	0.05895 (1,4)	1.497 (2,3)	1.332 (3,2)
	AIC					
	CHAA for liver			CHAA for kidney		
Simpler model	Linear regression through origin			Linear regression through origin		
Probability it is correct	98.95%	>99.99%	N.A.	99.30%	>99.99%	N.A.
Alternative model	Linear	Quadratic	Cubic[a]	Linear	Quadratic	Cubic[a]
Probability it is correct	1.05%	<0.01%	N.A.	0.70%	<0.01%	N.A.
Ratio of probabilities	94.29		N.A.	142.04		N.A.
Preferred model	Linear regression through origin			Linear regression through origin		
Difference in corrected AIC	−9.093	−31.04	N.A.	−9.912	−35.85	N.A.

[a] Cannot be calculated due to too few points.

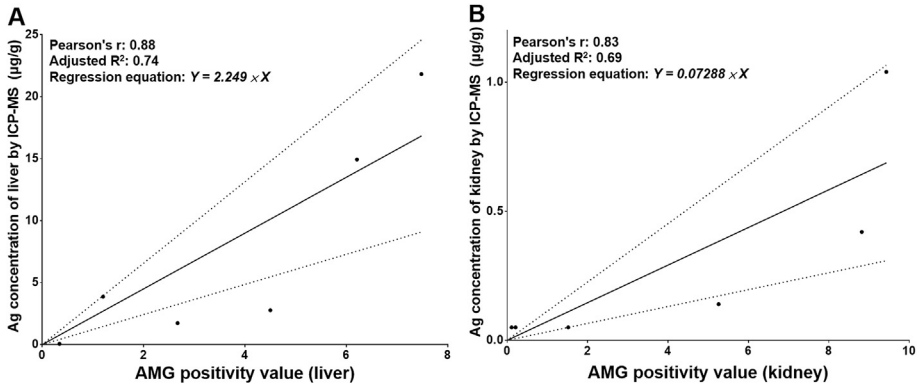

Fig. 3. Linear regression through origin for estimated Ag concentrations in the (A) liver and (B) kidney of 6 cetaceans (2 *Kogia* spp., 1 *Grampus griseus*, 2 *Lagenodelphis hosei* and 1 *Stenella attenuata*) with known Ag concentrations from autometallography positivity values. 95% confidence bands of the best-fit line of the regression line are shown as a dotted line.

concentrations of the kidney tissues were higher than the unhealthy Ag concentration (Fig. 4E).

3.4. Histopathological findings in liver and kidney tissues with different estimated silver concentrations

A variety of lesions were observed in the liver and kidney tissues of stranded cetaceans. The lesions found in liver tissues included hyaline inclusion (n = 58), non-specific reactive hepatitis (n = 51), severe congestion (n = 38), vacuolar degeneration (n = 37), multifocal necrosis (n = 2), extramedullary hematopoiesis (n = 2), periportal fibrosis (n = 2), and fibrotic nodule (n = 1). On the other hand, vacuolar degeneration of the proximal renal tubular epithelium (n = 10), hyaline droplets in the proximal renal tubular epithelium (n = 9), interstitial nephritis (n = 3), glomerulonephropathy (n = 2), interstitial fibrosis (n = 2), pyelonephritis (n = 2), suppurative nephritis (n = 1) were found in the kidney tissues. However, no lesions with marked intralesional aggregates of AMG positive signals were observed. The lesions with >3 frequencies (n > 3) were used in the correlation analysis, but there was no statistically significant correlation between these lesions and Ag concentrations. The frequencies and percentages of lesions presented in the liver and kidney tissues with baseline, intermediate and high Ag concentrations were summarized in Table 5.

4. Discussion

After intravenous injection of dextrin-silver colloid in laboratory rats, Ag was largely distributed in the spleen, liver and bone marrow, but the exact location of Ag deposition on the suborgan and cell levels was still undetermined (Gammill et al., 1950). Afterward, the technique of AMG for visualizing the metal elements with light and electron microscopy was described in 1981, and that technique has been improved with specific procedures over the years to detect different trace metals in various tissues of humans and animals (Dimitriadis et al., 2003; Loumbourdis and Danscher, 2004; Miller et al., 2016; Stoltenberg et al., 2003; Zarnescu et al., 2017; Zhu et al., 2012). The use of AMG to detect Ag in Wistar rats with intraperitoneal injection of silver lactate demonstrated the suborgan and cell level distributions of Ag, including 1) lysosomes of proximal renal tubular epithelium, mesangial cells, hepatocytes, macrophages (such as Kupffer cells and glial cells) and motor neurons; 2) basal lamina (a portion of basement membrane) of glomeruli, renal tubules, epidermis, and mucosal epithelium of tongue; 3) interstitium of renal papilla; 4) pheochromocytes of adrenal glands (Danscher, 1981). The AMG positive signals in F334

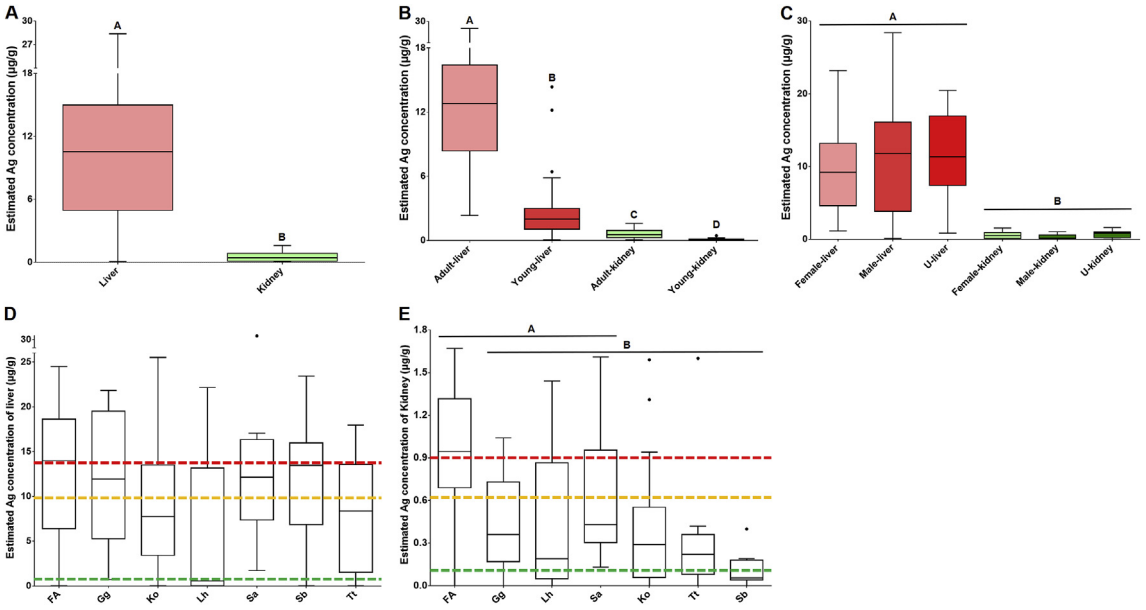

Fig. 4. Ag concentrations of cetacean tissues divided by different parameters, including (A) sample type (livers and kidneys), (B) age classes and sample type, (C) sex and sample type, (D) and (E) species and sample types. Fa = *Feresa attenuata*, Gg = *Grampus griseus*, Ko = *Kogia* spp., Lh = *Lagenodelphis hosei*, Sa = *Stenella attenuata*, Sb = *Steno bredanensis*, Tt = *Tursiops truncatus*. The bar in the middle of the box represents the median, and the bottom and top of the box describe the first and third quartiles. The whiskers show the 75th percentile plus 1.5 times IQR and 25th percentile minus 1.5 times IQR of all data, and any values greater than these are defined as outliers and plotted as individual points. Significant differences between groups at $p < .05$, Mann-Whitney *U* test (Fig. 3A) or Kruskal-Wallis Test (Fig. 3B–E) are indicated by different letters. The green, yellow, and red dashed lines indicate the upper limits of the baseline, and unhealthy and critically dangerous concentrations of Ag in the liver and kidney tissues of cetaceans. (For interpretation of the references to colour in this figure legend, the reader is referred to the Web version of this article.)

rats with oral administration of AgNPs (60 nm in diameter) were golden-yellow to brown positive signals and mainly located in the basement membranes of renal tubules, glomeruli, and transitional epithelium of the urinary bladder (Kim et al., 2009). A previous study also demonstrated that AMG positive signals (black dots) were observed in alveolar macrophages, ependymal cells, the choroid plexus, and the perivascular regions of the lung and renal cortex in laboratory rats after intranasal exposure of AgNPs (18–19 nm in diameter) (Miller et al., 2016).

It is evident that Ag can bind to metallothionein (MT), selenium (Se) and high-molecular-weight substances (HMWS) in the livers of cetaceans and mainly accumulates in nuclear, lysosomal, and mitochondrial fractions, as shown by cell fractionation analysis (Ikemoto et al., 2004a, b; Kunito et al., 2004). In the present study, the AMG positive signals in the liver tissues of cetaceans were brown to black dots in hepatocytes and Kupffer cells, similar to the results of a previous study conducted in 1981 (Danscher, 1981). Therefore, it is presumed that Ag is conjugated with MT, Se and HMWS, and then mainly accumulates in lysosomes of hepatocytes of cetaceans. The AMG positivity signals in the kidney tissues of cetaceans were mainly located in the proximal renal tubules of the renal cortex. A previous study applied autofluorescent signals and immunohistochemistry to localize Ag-MT complexes in the kidneys of laboratory rats with intraperitoneal injection of silver lactate, and it was found that they were exclusively located in the proximal renal tubules of the renal cortex (Kurasaki et al., 2000). Previous studies have indicated that the proximal renal tubular epithelium of S1 and S2 segments have active endocytosis with abundant intracytoplasmic lysosomes, and heavy metals can be uptaken by tubular epithelium via endocytosis (Barbier et al., 2005; Cristofori et al., 2007). Therefore, our findings may suggest that Ag/Ag compounds in cetacean kidneys are reabsorbed by the proximal renal tubular epithelium.

Our study also found differences in the AMG positive signals as compared to previous studies (Danscher, 1981; Kim et al., 2009). Since the basement membrane was considered the major location of Ag deposition after oral administration of $AgNO_3$ in laboratory rats (Boudreau et al., 2016; McGiven et al., 1977; Walker, 1972), it was surprising that the AMG positivity signals in the basement membrane of renal tubules and glomeruli were rarely found in kidney tissues of cetaceans. Although the mechanism of Ag deposition in the basement membrane is still largely unknown, it can be associated with the high affinity of Ag to the abundant negative-charged sulfhydryl and/or disulfide groups in the basement membrane (Boudreau et al., 2016; Walker, 1971, 1972). Furthermore, in previous studies, AMG positivity signals were observed in the nucleus of the interstitial cells of the inner renal medulla (Kim et al., 2009), but not in our study. The above differences indicate that the metabolic profile of Ag in cetaceans is different from that in laboratory rats.

The underlying mechanisms that cause the different metabolic profile of Ag in cetaceans are still undetermined, but several possibilities should be considered. First, cetaceans may have different physiological characteristics, and the composition of the basement membrane in cetaceans could be different from those of laboratory rats or other animals. Second, cetaceans may be exposed to different types of Ag/Ag compounds, which could be quite different from the Ag/Ag compounds used in previous studies on laboratory animals. Third, cetaceans are exposed to varieties of contaminants; thus, the interactions between Ag/Ag compounds and other contaminants in cetaceans may also affect the process of Ag deposition. In addition, cetaceans may expose to Ag/Ag compounds at extremely low concentration and for relatively long period of time, which are different from laboratory animals and may affect the process of Ag deposition.

Based on the significantly higher concentrations and diffuse distribution patterns of Ag in the livers of these seven cetacean species, it is most likely that the liver is the main storage organ for

Table 4
Silver (Ag) concentrations (mean ± stand deviation, μg/g dry wt.) of the liver and kidney tissues of cetaceans in various studies worldwide.

Location	Oceans	Time period	Species	Liver		Kidney		References
				N	Mean ± SD	N	Mean ± SD	
Alaska, US	Arctic	1989–1990	*Delphinapterus leucas*	14	86.44 ± 83.63[a]	–	–	(Becker et al., 1995)
Alaska, US	Arctic	1989–1990	*Globicephala melas*	8	0.53 ± 0.36[a]	–	–	(Becker et al., 2000)
Alaska, US	Arctic	1992–1999	*Delphinapterus leucas*	48	42.37 ± 29.3[a]	–	–	(Dehn et al., 2006; Woshner et al., 2001)
Alaska, US	Arctic	1983–2001	*Balaena mysticetus*	127	0.43 ± 0.93[a]	–	–	(Dehn et al., 2006; RJ et al., 1995; Woshner et al., 2001)
Alaska, US	Arctic	1983–2001	*Balaena mysticetus*	82	0.46 ± 1.09[a]	86	0.04 ± 0.04[a]	(Rosa et al., 2008)
Spain	North Atlantic	2004–2008	*Delphinus delphis*	100	0.69 ± 0.69[a]	98	<0.31[a]	(Mendez-Fernandez et al., 2014)
Spain	North Atlantic	2004–2009	*Globicephala melas*	8	0.43 ± 0.69[a]	6	<0.31[a]	(Mendez-Fernandez et al., 2014)
Spain	North Atlantic	2004–2010	*Phocoena phocoena*	14	3.44 ± 3.5[a]	12	<0.31[a]	(Mendez-Fernandez et al., 2014)
Spain	North Atlantic	2004–2011	*Stenella coeruleoalba*	18	0.99 ± 0.99[a]	16	<0.31[a]	(Mendez-Fernandez et al., 2014)
Spain	North Atlantic	2004–2012	*Tursiops truncatus*	8	0.66 ± 0.63[a]	6	<0.31[a]	(Mendez-Fernandez et al., 2014)
Carolina, US	North Atlantic	1990–2011	*Kogia sima*	12	3.12 ± 1.06[a]	9	N.D.	(Reed et al., 2015)
Argentina	South Atlantic	2010–2011	*Cephalorhynchus commersonii*	7	5.4 ± 5	6	1.2 ± 2.7	(Caceres-Saez et al., 2013)
Brazil	South Atlantic	1997–2002	*Delphinus capensis*	1	2.71[a]	–	–	(Kunito et al., 2004)
Brazil	South Atlantic	1997–2000	*Pontoporia blainvillei*	23	7.93 ± 13.54[a]	–	–	(Kunito et al., 2004)
Brazil	South Atlantic	1997–1999	*Sotalia guianensis*	20	6.28 ± 4.29[a]	–	–	(Kunito et al., 2004)
Brazil	South Atlantic	1997–2003	*Stenella coeruleoalba*	1	10.57[a]	–	–	(Kunito et al., 2004)
Brazil	South Atlantic	1997–2001	*Stenella frontalis*	2	4.96[a]	–	–	(Kunito et al., 2004)
Brazil	South Atlantic	N.A.	*Sotalia guianensis*	19	0.79 ± 0.89	–	–	(Seixas et al., 2009)
Alaska, US	North Pacific	1992–1996	*Delphinapterus leucas*	6	22.4 ± 13.78[a]	–	–	(Becker et al., 2000)
Taiwan	North Pacific	1994–1995	*Grampus griseus*	2	0.46 ± 0.12	–	–	(Chen et al., 2017)
Taiwan	North Pacific	2001–2012	*Grampus griseus*	12	5.87 ± 10.80	12	0.19 ± 0.22	(Chen et al., 2017)
Taiwan	North Pacific	2001–2012	*Kogia simus*	–	–	6	0.28 ± 0.36	(Chen et al., 2017)
Taiwan	North Pacific	1994–1995	*Stenella attenuata*	4	0.42 ± 0.16	–	–	(Chen et al., 2017)
Taiwan	North Pacific	2001–2012	*Stenella attenuata*	9	1.45 ± 1.99	10	0.24 ± 0.20	(Chen et al., 2017)
Russia	North Pacific	2001	*Eschrichtius robustus*	29	0.33 ± 0.46[a]	–	–	(Dehn et al., 2006)
Japan	North Pacific	1997–1998	*Phocoenoides dalli*	6	4.29 ± 3.63	6	–	(Ikemoto et al., 2004a)
Russia	North Pacific	1994	*Eschrichtius robustus*	5	1.02 ± 0.2[a]	–	–	(Tilbury et al., 2002)
Taiwan	North Pacific	1999–2016	*Feresa attenuata*	22	12.95 ± 6.64	22	0.91 ± 0.43	This study
Taiwan	North Pacific	1999–2016	*Grampus griseus*	5	12.67 ± 7.09	5	0.43 ± 0.36	This study
Taiwan	North Pacific	1999–2016	*Kogia* spp.	38	9.32 ± 6.08	38	0.38 ± 0.36	This study
Taiwan	North Pacific	1999–2016	*Lagenodelphis hosei*	13	6.96 ± 6.87	13	0.44 ± 0.46	This study
Taiwan	North Pacific	1999–2016	*Stenella attenuata*	13	12.65 ± 6.28	13	0.63 ± 0.44	This study
Taiwan	North Pacific	1999–2016	*Steno bredanensis*	8	11.89 ± 6.13	8	0.14 ± 0.13	This study
Taiwan	North Pacific	1999–2016	*Tursiops truncatus*	11	9.27 ± 5.6	11	0.33 ± 0.42	This study
New Zealand	South Pacific	1999–2005	*Delphinus capensis*	3	2.65 ± 0.99[a]	3	0.15 ± 0[a]	(Stockin et al., 2007)

[a] Wet weight basis concentration has been converted to dry weight basis concentration by assuming that moisture content was 69.73% for liver and 77.32 for kidney (Yang and Miyazaki, 2003).

Table 5
The lesions presented in the liver and kidney tissues of stranded cetaceans with high, intermediate and baseline Ag concentrations.

Lesions[a]		Ag concentration[b]			
		High N = 83	Intermediate N = 24	Baseline N = 3	Significance[d]
Liver[e]	Severe congestion	31 (42.5%)	7 (29.2%)	0 (0.0%)	NS
	Vacuolar degeneration of hepatocytes	29 (33.3%)	7 (29.2%)	1 (33.3%)	NS
	Non-specific reactive hepatitis	41 (47.1%)	10 (41.7%)	0 (0.0%)	NS
	Hyaline inclusions in hepatocytes	47 (54.0%)	9 (37.5%)	2 (66.7%)	NS
Lesions[a]		Ag concentration[c]			
		High N = 60	Intermediate N = 27	Baseline N = 23	Significance[d]
Kidney	Vacuolar degeneration of proximal renal tubular epithelium	5 (8.3%)	3 (11.1%)	2 (8.7%)	NS
	Hyaline droplets in the proximal renal tubular epithelium	11 (19.3%)	4 (14.8%)	4 (17.4%)	NS

[a] The lesions with >3 frequencies (n > 3) were used in the correlation analysis.
[b] The liver tissues with estimated Ag concentrations ≤0.43, 0.43–4.45, and ≥4.45 μg/g were respectively classified into baseline, intermediate, and high group (Chen et al., 2017).
[c] The kidney tissues with estimated Ag concentrations ≤0.08, 0.08–0.33, and ≥0.33 μg/g were respectively classified into baseline, intermediate, and high groups (Chen et al., 2017).
[d] p-value < .05 was considered statistically significant. NS = No significance.
[e] Because the observed values were less than 5 in some cells of the contingency table, Fisher's exact test was used.

Ag/Ag compounds, but the kidneys may be a transit station for the metabolism of Ag/Ag compounds in cetaceans. Although the metabolism of Ag is still largely unknown in animals, a presumptive metabolic pathway of Ag in cetaceans is advanced based on our results and previous studies focused on heavy metals metabolism (Fig. 5). It is presumed that Ag/Ag compounds can enter the cetacean body through food intake and then be delivered to the liver through the gastrointestinal tract and portal circulation (Loeschner et al., 2011; van der Zande et al., 2012). Previous studies found that Ag can bind to the Se and HMWS, and Se is a component of the

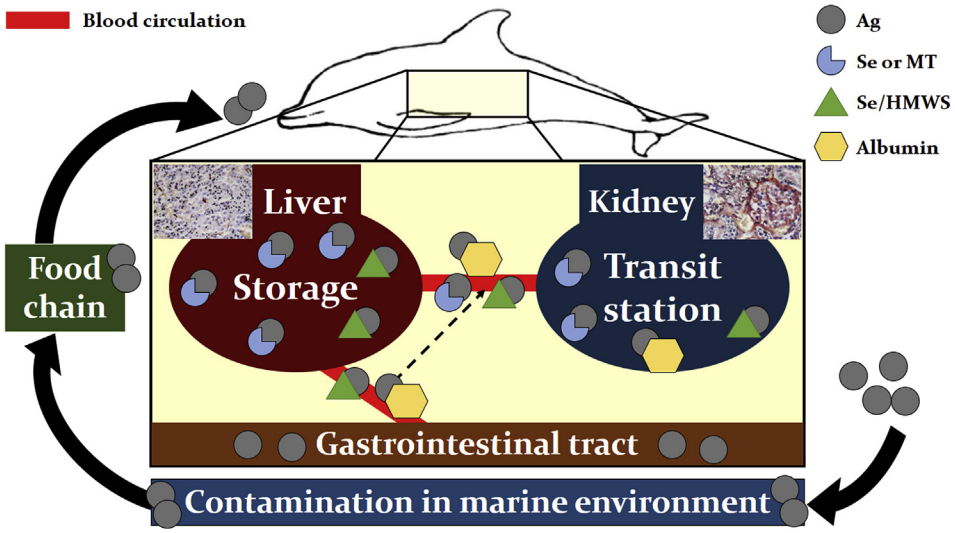

Fig. 5. Presumptive metabolic pathway of Ag in cetaceans. Se = selenium; MT = metallothionein; HMWS = high-molecular-weight substances.

HMWS in plasma protein (Ikemoto et al., 2004a; Naganuma and Imura, 1983; Yoneda and Suzuki, 1997a, b). Besides, previous studies also suggested that the heavy metals can bind rapidly to albumin in plasma (Barbier et al., 2005). Therefore, the Ag/Ag compounds during the portal circulation is considered to be conjugated with proteins, including Se, HMWS or albumin. Most of the Ag/Ag compounds with proteins (Se, HMWS or albumin) conjugation are uptaken by hepatocytes, degraded in lysosomes, released into the cytoplasm of hepatocytes, conjugated with MT, Se or HMWS, and stored in the lysosomes of hepatocytes (Ikemoto et al., 2004a, b; Kunito et al., 2004). Some of the Ag/Ag compounds with protein (Se, HMWS or albumin) conjugation may still remain in blood circulation, or those with MT, Se or HWMS conjugation in hepatocytes may be released into blood circulation during renewal of hepatocytes (Barbier et al., 2005; Loeschner et al., 2011; van der Zande et al., 2012). The Ag/Ag compounds in blood circulation can be subsequently delivered to multiple organs, such as the kidneys (Loeschner et al., 2011; van der Zande et al., 2012). In the kidneys, Ag/Ag compounds with MT, Se, HWMS or albumin conjugation can penetrate through the glomeruli and then be reabsorbed by proximal renal tubular epithelium (Barbier et al., 2005; Cristofori et al., 2007; Kurasaki et al., 2000).

The significant positive correlation between the results of ICP-MS and AMG positivity values suggests that the areas of AMG positivity signals can be a parameter for estimating the Ag concentration. Therefore, the CHAA was developed based on the AMG positivity values and regression model. Generally, a more complicated model with more parameters fits the data better than the simpler one (in other words, it has a relatively high adjusted R^2), but it is necessary to statistically evaluate whether the differences among these regression models are sufficient to justify a preference for the more complicated model. Hence, these regression models were compared statistically (Liang et al., 2017; Spiess and Neumeyer, 2010), and the results showed that linear regression through origin was preferred for the CHAA in both the livers and kidneys of cetaceans. The adjusted R^2 of the CHAA for livers (0.74) and kidneys (0.69) indicates that most of the response is attributed to Ag concentration, but some undetermined factors still influence the CHAA for the liver and kidney tissues of cetaceans. One of the possible factors influencing the CHAA for the liver and kidney tissues of cetaceans is the differences among cetacean species. The samples with known Ag concentrations in the current study were collected from cetaceans of four different species, which have different habitats, prey, and physiological characteristics (Baird, 2009; Louella and Dolar, 2009; McAlpine, 2009; Perrin, 2009). Therefore, it is rational to consider that the models for estimating the Ag concentration by AMG positivity values may be different for different cetacean species. The best way to improve the effect size (adjusted R^2) of our models is to increase the sample sizes of each cetacean species with known Ag concentrations determined by ICP-MS. Furthermore, if the sample sizes are large enough, more accurate models for estimating the Ag concentration can be developed for each cetacean species.

Considering the mean SDs of the accuracy tests of the CHAA (liver: 3.24; kidney: 0.16) and the precision tests of the semi-quantitative analysis for AMG positivity (liver: 2.8; kidney: 0.35), the accuracy errors of the CHAA may be largely attributable to the errors in the semi-quantitative analysis for AMG positivity. In particular, the mean SD in the precision test of the semi-quantitative analysis in the kidney tissues of cetaceans is larger than that of the accuracy test in the CHAA for kidneys ($0.35 > 0.16$). Therefore, the accuracy of the CHAA for kidneys may be lower than that for livers, and it might be associated with the uneven distribution of the AMG positivity signals and the relatively low Ag concentrations in the kidney tissues of cetaceans. In contrast, the accuracy of the CHAA for livers is not affected by the above factors because of the even distribution of AMG positive signals and the relatively high Ag concentrations in the liver tissues of cetaceans. This phenomenon also explains the relatively lower adjusted R^2 in the CHAA for kidneys, and the reliability of the CHAA for kidneys is low.

Intracytoplasmic hyaline inclusions of hepatocytes were commonly found in the stranded cetaceans of each species in this study. The hyaline inclusions are most likely associated with hepatocellular hypoxia due to impaired blood circulation during stranding, but other possibilities such as morbillivirus infection and toxic effect of contaminants have been postulated (Jaber et al., 2004). Non-specific reactive hepatitis, characterized by infiammatory cells infiltrations in portal areas and/or in the parenchyma without the presence of hepatocellular necrosis, represents a non-specific response to the extrahepatic diseases and/or previous intrahepatic inflammatory diseases (Jaber et al., 2004; van den Ingh et al., 2006). Severe congestion of liver is most frequently observed in the *Kogia* spp. (34/38), and this lesion has been associated with

dilated cardiomyopathy in this species (Bossart et al., 1985, 2007). Vacuolar degeneration of hepatocytes is not uncommon in stranded cetaceans with metabolic disorders due toxic injuries and/or nutritional deficiencies (Jaber et al., 2004). The meanings of hyaline droplets and vacuolar degeneration of renal tubular epithelium in cetaceans are still undetermined. In laboratory rats and mice, the presence of hyaline droplets indicated that the low molecular weight protein is accumulated within lysosomes due to impairment of tubular reabsorption/hydrolysis, which is as associated with increased filtered protein loads or decreased catabolism (Frazier et al., 2012). The vacuolar degeneration of proximal renal tubular epithelium may be a preceding and reversible change of tubular degeneration/necrosis, but may be a post-mortem change and can be observed in healthy animals (Frazier et al., 2012). As above, the lesions found in liver and kidney tissues are non-specific, and no marked intralesional aggregates of AMG positive signals are noted. Besides, there was no statistically significant correlation between these lesions and Ag concentrations of liver and kidney tissues of cetaceans, and thus there is no direct evidence of Ag deposition induced lesions in the liver and kidney tissues of cetaceans. However, stranded cetaceans are not laboratory animals and not well controlled to expose to a single contaminant. Therefore, further investigations are warranted to study the systemic Ag distribution, the cause of death/stranding, and the infectious diseases in stranded cetaceans with different Ag concentrations for comprehensively evaluating the negative health effects caused by Ag in cetaceans.

Although there is no statistically significant correlation between the observed lesions and Ag concentrations in the liver and kidney tissues, the Ag concentrations of cetaceans in the present study are relatively higher than those reported in previous studies conducted in other marine regions, with the exceptions of *Delphinapterus leucas* in the Arctic Ocean and *Sotalia guianensis* and *Pontoporia blainvillei* in the South Atlantic Ocean (Table 4). The Ag concentrations found in the present study also indicate that Ag contamination is relatively more severe in the North-western Pacific Ocean than in other marine regions of the world. In addition, most of the estimated Ag concentrations in the liver and kidney tissues of stranded cetaceans in Taiwan are markedly higher than the baseline concentrations (Chen et al., 2017), and this finding further suggests that the Ag contamination in the North-western Pacific Ocean may have caused detrimental effects on the health of cetaceans.

In addition, a significant age-dependent increase in the Ag concentration estimated by the CHAA was found in the present study, and similar phenomena have been reported in a variety of cetacean species (Becker et al., 1995; Reed et al., 2015; Romero et al., 2017; Seixas et al., 2009). This data indicates that the Ag deposition in cetaceans aggravate with time, and thus the source of Ag deposition is most likely from their prey. The tissues of cetaceans in this study were from 7 different species and have different habitats and prey, but there are no significant difference in Ag concentrations between different cetacean species. This finding also suggests that the Ag contamination may exist in all aspects of the marine ecosystem. Therefore, it is necessary to raise the public awareness and encourage more studies about Ag contamination.

5. Conclusions

In summary, the present study localized Ag by AMG and developed a model called the CHAA to estimate the Ag concentrations in liver and kidney tissues from 7 cetacean species. The Ag distribution pattern in cetaceans was different from those in previous studies conducted in laboratory rats, and this difference may suggest that cetaceans have a different metabolic profile of Ag. Therefore, a presumptive metabolic pathway of Ag in cetaceans is advanced. Furthermore, our results suggest that Ag contamination is more severe in cetaceans living in the North-western Pacific Ocean than in cetaceans living in other marine regions of the world and may have detrimental effects on their health condition.

Declaration of interest statement

The authors report no conflicts of interest.

Acknowledgments

We thank the Taiwan Cetacean Stranding Network for sample collection and storage, including the Taiwan Cetacean Society, Taipei; the Cetacean Research Laboratory (Prof. Lien-Siang Chou), the Institute of Ecology and Evolutionary Biology, National Taiwan University, Taipei; the National Museum of Marine Biology and Aquarium (Dr. Chiou-Ju Yao), Taichung; and the Marine Biology & Cetacean Research Center, National Cheng-Kung University. This study is partially supported by the Ministry of Science & Technology, Taiwan under Grant MOST 106-2313-B-002-054-.

Appendix A. Supplementary data

Supplementary data related to this article can be found at https://doi.org/10.1016/j.envpol.2018.01.010.

References

Ajmal, C.M., Menamparambath, M.M., Choi, H.R., Baik, S., 2016. Extraordinarily high conductivity of flexible adhesive films by hybrids of silver nanoparticle-nanowires. Nanotechnology 27, 225603. https://doi.org/10.1088/0957-4484/27/22/225603.

Anderson, D.S., Patchin, E.S., Silva, R.M., Uyeminami, D.L., Sharmah, A., Guo, T., Das, G.K., Brown, J.M., Shannahan, J., Gordon, T., Chen, L.C., Pinkerton, K.E., Van Winkle, L.S., 2015. Influence of particle size on persistence and clearance of aerosolized silver nanoparticles in the rat lung. Toxicol. Sci. 144, 366–381. https://doi.org/10.1093/toxsci/kfv005.

Baird, R.W., 2009. Risso's dolphin: Grampus griseus. In: Perrin, William F., Würsig, B., Thewissen, J.G.M. (Eds.), Encyclopedia of Marine Mammals, second ed. Academic Press, London, pp. 975–976.

Barbier, O., Jacquillet, G., Tauc, M., Cougnon, M., Poujeol, P., 2005. Effect of heavy metals on, and handling by, the kidney. Nephron. Physiol. 99, p105–110. https://doi.org/10.1159/000083981.

Becker, P., Krahn, M., Mackey, E., Demiralp, R., Schantz, M., Epstein, M., Donais, M., Porter, B., Muir, D., Wise, S., 2000. Concentrations of Polychlorinated Biphenyls (PCB's) Chlorinated Pesticides and Heavy Metals and Other Elements in Tissues of Belugas *Delphinapterus leucas* from Cook Inlet Alaska.

Becker, P.R., Mackey, E.A., Demiralp, R., Suydam, R., Early, G., Koster, B.J., Wise, S.A., 1995. Relationship of silver with selenium and mercury in the liver of two species of toothed whales (odontocetes). Mar. Pollut. Bull. 30, 262–271. https://doi.org/10.1016/0025-326X(94)00176-A.

Bischoff, K., Lamm, C., Erb, H.N., Hillebrandt, J.R., 2008. The effects of formalin fixation and tissue embedding of bovine liver on copper, iron, and zinc analysis. J. Vet. Diagn. Invest. 20, 220–224. https://doi.org/10.1177/104063870802000213.

Bonta, M., Torok, S., Hegedus, B., Dome, B., Limbeck, A., 2017. A comparison of sample preparation strategies for biological tissues and subsequent trace element analysis using LA-ICP-MS. Anal. Bioanal. Chem. 409, 1805–1814. https://doi.org/10.1007/s00216-016-0124-6.

Bornhorst, J.A., Hunt, J.W., Urry, F.M., McMillin, G.A., 2005. Comparison of sample preservation methods for clinical trace element analysis by inductively coupled plasma mass spectrometry. Am. J. Clin. Pathol. 123, 578–583. https://doi.org/10.1309/L241-WUER-8831-GLWB.

Bossart, G.D., 2011. Marine mammals as sentinel species for oceans and human health. Vet. Pathol. 48, 676–690. https://doi.org/10.1177/0300985810388525.

Bossart, G.D., Hensley, G., Goldstein, J.D., Kroell, K., Manire, C.A., Defran, R.H., Reif, J.S., 2007. Cardiomyopathy and myocardial degeneration in stranded pygmy (*Kogia breviceps*) and dwarf (*Kogia sima*) sperm whales. Aquat. Mamm. 33, 214–222. https://doi.org/10.1578/AM.33.2.2007.214.

Bossart, G.D., Odell, D.K., Altman, N.H., 1985. Cardiomyopathy in stranded pygmy and dwarf sperm whales. J. Am. Vet. Med. Assoc. 187, 1137–1140.

Boudreau, M.D., Imam, M.S., Paredes, A.M., Bryant, M.S., Cunningham, C.K., Felton, R.P., Jones, M.Y., Davis, K.J., Olson, G.R., 2016. Differential effects of silver nanoparticles and silver ions on tissue accumulation, distribution, and toxicity in the Sprague Dawley rat following daily oral gavage administration for 13

weeks. Toxicol. Sci. 150, 131–160. https://doi.org/10.1093/toxsci/kfv318.
Buffet, P.E., Zalouk-Vergnoux, A., Chatel, A., Berthet, B., Metais, I., Perrein-Ettajani, H., Poirier, L., Luna-Acosta, A., Thomas-Guyon, H., Risso-de Faverney, C., Guibbolini, M., Gilliland, D., Valsami-Jones, E., Mouneyrac, C., 2014. A marine mesocosm study on the environmental fate of silver nanoparticles and toxicity effects on two endobenthic species: the ragworm *Hediste diversicolor* and the bivalve mollusc *Scrobicularia plana*. Sci. Total Environ. 470–471, 1151–1159. https://doi.org/10.1016/j.scitotenv.2013.10.114.
Caceres-Saez, I., Ribeiro Guevara, S., Dellabianca, N.A., Goodall, R.N., Cappozzo, H.L., 2013. Heavy metals and essential elements in Commerson's dolphins (*Cephalorhynchus c. commersonii*) from the southwestern South Atlantic Ocean. Environ. Monit. Assess. 185, 5375–5386. https://doi.org/10.1007/s10661-012-2952-y.
Chen, M.H., Shih, C.C., Chou, C.L., Chou, L.S., 2002. Mercury, organic-mercury and selenium in small cetaceans in Taiwanese waters. Mar. Pollut. Bull. 45, 237–245. https://doi.org/10.1016/S0025-326X(02)00095-4.
Chen, M.H., Zhuang, M.F., Chou, L.S., Liu, J.Y., Shih, C.C., Chen, C.Y., 2017. Tissue concentrations of four Taiwanese toothed cetaceans indicating the silver and cadmium pollution in the western Pacific Ocean. Mar. Pollut. Bull. https://doi.org/10.1016/j.marpolbul.2017.03.028.
Cristofori, P., Zanetti, E., Fregona, D., Piaia, A., Trevisan, A., 2007. Renal proximal tubule segment-specific nephrotoxicity: an overview on biomarkers and histopathology. Toxicol. Pathol. 35, 270–275. https://doi.org/10.1080/01926230601187430.
Danscher, G., 1981. Light and electron microscopic localization of silver in biological tissue. Histochemistry 71, 177–186.
Danscher, G., 1991. Applications of autometallography to heavy metal toxicology. Pharmacol. Toxicol. 68, 414–423.
Dehn, L.A., Follmann, E.H., Thomas, D.L., Sheffield, G.G., Rosa, C., Duffy, L.K., O'Hara, T.M., 2006. Trophic relationships in an Arctic food web and implications for trace metal transfer. Sci. Total Environ. 362, 103–123. https://doi.org/10.1016/j.scitotenv.2005.11.012.
Deroulers, C., Ameisen, D., Badoual, M., Gerin, C., Granier, A., Lartaud, M., 2013. Analyzing huge pathology images with open source software. Diagn. Pathol. 8 https://doi.org/10.1186/1746-1596-8-92, 92.
Dimitriadis, V.K., Domouhtsidou, G.P., Raftopoulou, E., 2003. Localization of Hg and Pb in the palps, the digestive gland and the gills in *Mytilus galloprovincialis* (L.) using autometallography and X-ray microanalysis. Environ. Pollut. 125, 345–353. https://doi.org/10.1016/S0269-7491(03)00122-2.
Farre, M., Gajda-Schrantz, K., Kantiani, L., Barcelo, D., 2009. Ecotoxicity and analysis of nanomaterials in the aquatic environment. Anal. Bioanal. Chem. 393, 81–95. https://doi.org/10.1007/s00216-008-2458-1.
Frazier, K.S., Seely, J.C., Hard, G.C., Betton, G., Burnett, R., Nakatsuji, S., Nishikawa, A., Durchfeld-Meyer, B., Bube, A., 2012. Proliferative and nonproliferative lesions of the rat and mouse urinary system. Toxicol. Pathol. 40, 14S–86S. https://doi.org/10.1177/0192623312438736.
Gammill, J.C., Wheeler, B., Carothers, E.L., Hahn, P.F., 1950. Distribution of radioactive silver colloids in tissues of rodents following injection by various routes. Proc Soc Exp Biol Med 74, 691–695.
Ge, L., Li, Q., Wang, M., Ouyang, J., Li, X., Xing, M.M., 2014. Nanosilver particles in medical applications: synthesis, performance, and toxicity. Int. J. Nanomed. 9, 2399–2407. https://doi.org/10.2147/IJN.S55015.
Geraci, J.R., Lounsbury, V.J., 2005. Specimen and data collection, marine mammals ashore: a field guide for strandings. Natl. Aquarium Baltimore 167–230.
Hansen, S.F., Heggelund, L.R., Besora, P.R., Mackevica, A., Boldrin, A., Baun, A., 2016. Nanoproducts - what is actually available to European consumers? Environ. Sci. -Nano 3, 169–180. https://doi.org/10.1039/c5en00182j.
Hohn, A.A., 2009. Age estimation. In: Würsig, B., Thewissen, J.G.M. (Eds.), Encyclopedia of Marine Mammals, second ed. Academic Press, London, pp. 11–17.
Ikemoto, T., Kunito, T., Anan, Y., Tanaka, H., Baba, N., Miyazaki, N., Tanabe, S., 2004a. Association of heavy metals with metallothionein and other proteins in hepatic cytosol of marine mammals and seabirds. Environ. Toxicol. Chem. 23, 2008–2016. https://doi.org/10.1897/03-456.
Ikemoto, T., Kunito, T., Tanaka, H., Baba, N., Miyazaki, N., Tanabe, S., 2004b. Detoxification mechanism of heavy metals in marine mammals and seabirds: interaction of selenium with mercury, silver, copper, zinc, and cadmium in liver. Arch. Environ. Contam. Toxicol. 47, 402–413. https://doi.org/10.1007/s00244-004-3188-9.
Jaber, J.R., Perez, J., Arbelo, M., Andrada, M., Hidalgo, M., Gomez-Villamandos, J.C., Van Den Ingh, T., Fernandez, A., 2004. Hepatic lesions in cetaceans stranded in the Canary Islands. Vet. Pathol. 41, 147–153. https://doi.org/10.1354/vp.41-2-147.
Jensen, E.C., 2013. Quantitative analysis of histological staining and fluorescence using ImageJ. Anat. Rec. -Adv. Integrat. Anat. Evol. Biol. 296, 378–381. https://doi.org/10.1002/ar.22641.
Kim, W.Y., Kim, J., Park, J.D., Ryu, H.Y., Yu, I.J., 2009. Histological study of gender differences in accumulation of silver nanoparticles in kidneys of Fischer 344 rats. J. Toxicol. Environ. Health A 72, 1279–1284. https://doi.org/10.1080/15287390903212287.
Kokkat, T.J., Patel, M.S., McGarvey, D., LiVolsi, V.A., Baloch, Z.W., 2013. Archived formalin-fixed paraffin-embedded (FFPE) blocks: a valuable underexploited resource for extraction of DNA, RNA, and protein. Biopreserv. Biobanking 11, 101–106. https://doi.org/10.1089/bio.2012.0052.
Kunito, T., Nakamura, S., Ikemoto, T., Anan, Y., Kubota, R., Tanabe, S., Rosas, F.C., Fillmann, G., Readman, J.W., 2004. Concentration and subcellular distribution of trace elements in liver of small cetaceans incidentally caught along the Brazilian coast. Mar. Pollut. Bull. 49, 574–587. https://doi.org/10.1016/j.marpolbul.2004.03.009.
Kurasaki, M., Okabe, M., Saito, S., Yamanoshita, O., Hosokawa, T., Saito, T., 2000. Histochemical characterization of silver-induced metallothionein in rat kidney. J. Inorg. Biochem. 78, 275–281.
Levard, C., Hotze, E.M., Lowry, G.V., Brown Jr., G.E., 2012. Environmental transformations of silver nanoparticles: impact on stability and toxicity. Environ. Sci. Technol. 46, 6900–6914. https://doi.org/10.1021/es2037405.
Liang, C.S., Ho, P.S., Yen, C.H., Chen, C.Y., Kuo, S.C., Huang, C.C., Yeh, Y.W., Ma, K.H., Huang, S.Y., 2017. The relationship between the striatal dopamine transporter and novelty seeking and cognitive flexibility in opioid dependence. Prog Neuropsychopharmacol Biol Psychiatry 74, 36–42. https://doi.org/10.1016/j.pnpbp.2016.12.001.
Louella, M., Dolar, L., 2009. Fraser's dolphin: Lagenodelphis hosei. In: Würsig, B., Thewissen, J.G.M. (Eds.), Encyclopedia of Marine Mammals, second ed. Academic Press, London, pp. 469–471.
Loeschner, K., Hadrup, N., Qvortrup, K., Larsen, A., Gao, X., Vogel, U., Mortensen, A., Lam, H.R., Larsen, E.H., 2011. Distribution of silver in rats following 28 days of repeated oral exposure to silver nanoparticles or silver acetate. Part. Fibre Toxicol. 8, 18.
Loumbourdis, N.S., Danscher, G., 2004. Autometallographic tracing of mercury in frog liver. Environ. Pollut. 129, 299–304. https://doi.org/10.1016/j.envpol.2003.10.010.
Massarsky, A., Trudeau, V.L., Moon, T.W., 2014. Predicting the environmental impact of nanosilver. Environ. Toxicol. Pharmacol. 38, 861–873. https://doi.org/10.1016/j.etap.2014.10.006.
McAlpine, D.F., 2009. Pygmy and dwarf sperm whales: *Kogia breviceps* and *K. sima*. In: Würsig, B., Thewissen, J.G.M. (Eds.), Encyclopedia of Marine Mammals, second ed. Academic Press, London, pp. 936–938.
McGiven, A.R., Day, W.A., Hunt, J.S., 1977. Glomerular lesions in argyric NZB/NZW mice. Br. J. Exp. Pathol. 58, 57–62.
Mendez-Fernandez, P., Webster, L., Chouvelon, T., Bustamante, P., Ferreira, M., Gonzalez, A.F., Lopez, A., Moffat, C.F., Pierce, G.J., Read, F.L., Russell, M., Santos, M.B., Spitz, J., Vingada, J.V., Caurant, F., 2014. An assessment of contaminant concentrations in toothed whale species of the NW Iberian Peninsula: part II. Trace element concentrations. Sci. Total Environ. 484, 206–217. https://doi.org/10.1016/j.scitotenv.2014.03.001.
Miller, D.L., Yu, I.J., Genter, M.B., 2016. Use of autometallography in studies of nanosilver distribution and toxicity. Int. J. Toxicol. 35, 47–51. https://doi.org/10.1177/1091581815616602.
Naganuma, A., Imura, N., 1983. Mode of in vitro interaction of mercuric mercury with selenite to form high-molecular weight substance in rabbit blood. Chem. Biol. Interact. 43, 271–282.
Nowack, B., Krug, H.F., Height, M., 2011. 120 years of nanosilver history: implications for policy makers. Environ. Sci. Technol. 45, 1177–1183. https://doi.org/10.1021/es103316q.
Nuttall, K.L., Gordon, W.H., Ash, K.O., 1995. Inductively coupled plasma mass spectrometry for trace element analysis in the clinical laboratory. Ann. Clin. Lab. Sci. 25, 264–271.
Parlee, S.D., Lentz, S.I., Mori, H., MacDougald, O.A., 2014. Quantifying size and number of adipocytes in adipose tissue. Meth. Enzymol. 537, 93–122. https://doi.org/10.1016/B978-0-12-411619-1.00006-9.
Perrin, W.F., 2009. Pantropical spotted dolphin: Stenella attenuata. In: Würsig, B., Thewissen, J.G.M. (Eds.), Encyclopedia of Marine Mammals, second ed. Academic Press, London, pp. 819–821.
Polanowski, A.M., Robbins, J., Chandler, D., Jarman, S.N., 2014. Epigenetic estimation of age in humpback whales. Mol Ecol Resour 14, 976–987. https://doi.org/10.1111/1755-0998.12247.
Reed, L.A., McFee, W.E., Pennington, P.L., Wirth, E.F., Fulton, M.H., 2015. A survey of trace element distribution in tissues of the dwarf sperm whale (*Kogia sima*) stranded along the South Carolina coast from 1990-2011. Mar. Pollut. Bull. 100, 501–506. https://doi.org/10.1016/j.marpolbul.2015.09.005.
RJ, T., TL, W., EM, H., 1995. Toxicological Studies in Tissues of the Beluga Whale Delphinapterus leucas along Northern Alaska with an Emphasis on Public Health Implications of Subsistence Utilization. Final report to the Alaska Beluga Whale Committee. Department of Wildlife Management, North Slope Borough, Barrow, Alaska.
Romero, M.B., Polizzi, P., Chiodi, L., Robles, A., Das, K., Gerpe, M., 2017. Metals as chemical tracers to discriminate ecological populations of threatened Franciscana dolphins (Pontoporia blainvillei) from Argentina. Environ Sci Pollut Res Int 24, 3940–3950. https://doi.org/10.1007/s11356-016-7970-9.
Rosa, C., Blake, J.E., Bratton, G.R., Dehn, L.A., Gray, M.J., O'Hara, T.M., 2008. Heavy metal and mineral concentrations and their relationship to histopathological findings in the bowhead whale (*Balaena mysticetus*). Sci. Total Environ. 399, 165–178. https://doi.org/10.1016/j.scitotenv.2008.01.062.
Seixas, T.G., Kehrig, H.A., Di Beneditto, A.P., Souza, C.M., Malm, O., Moreira, I., 2009. Essential (Se, Cu) and non-essential (Ag, Hg, Cd) elements: what are their relationships in liver of *Sotalia guianensis* (Cetacea, Delphinidae)? Mar. Pollut. Bull. 58, 629–634. https://doi.org/10.1016/j.marpolbul.2008.12.005.
Shu, J., Dolman, G.E., Duan, J., Qiu, G., Ilyas, M., 2016. Statistical colour models: an automated digital image analysis method for quantification of histological biomarkers. Biomed. Eng. Online 15, 46. https://doi.org/10.1186/s12938-016-0161-6.
Spiess, A.N., Neumeyer, N., 2010. An evaluation of R2 as an inadequate measure for

nonlinear models in pharmacological and biochemical research: a Monte Carlo approach. BMC Pharmacol. 10, 6. https://doi.org/10.1186/1471-2210-10-6.
Stockin, K.A., Law, R.J., Duignan, P.J., Jones, G.W., Porter, L., Mirimin, L., Meynier, L., Orams, M.B., 2007. Trace elements, PCBs and organochlorine pesticides in New Zealand common dolphins (*Delphinus* sp.). Sci. Total Environ. 387, 333–345. https://doi.org/10.1016/j.scitotenv.2007.05.016.
Stoltenberg, M., Danscher, G., 2000. Histochemical differentiation of autometallographically traceable metals (Au, Ag, Hg, Bi, Zn): protocols for chemical removal of separate autometallographic metal clusters in Epon sections. Histochem. J. 32, 645–652.
Stoltenberg, M., Larsen, A., Kemp, K., Bloch, D., Weihe, P., 2003. Autometallographic tracing of mercury in pilot whale tissues in the Faroe Islands. Int. J. Circumpolar Health 62, 182–189. https://doi.org/10.3402/ijch.v62i2.17552.
Tilbury, K.L., Stein, J.E., Krone, C.A., Brownell Jr., R.L., Blokhin, S.A., Bolton, J.L., Ernest, D.W., 2002. Chemical contaminants in juvenile gray whales (*Eschrichtius robustus*) from a subsistence harvest in Arctic feeding grounds. Chemosphere 47, 555–564. https://doi.org/10.1016/S0045-6535(02)00061-9.
Tran, J.Q., Dranikov, A., Iannucci, A., Wagner, W.P., LoBello, J., Allen, J., Weiss, G.J., 2014. Heavy metal content in thoracic tissue samples from patients with and without NSCLC. Lung Canc. Int 2014, 853158. https://doi.org/10.1155/2014/853158.
Vance, M.E., Kuiken, T., Vejerano, E.P., McGinnis, S.P., Hochella Jr., M.F., Rejeski, D., Hull, M.S., 2015. Nanotechnology in the real world: redeveloping the nanomaterial consumer products inventory. Beilstein J. Nanotechnol. 6, 1769–1780. https://doi.org/10.3762/bjnano.6.181.
van den Ingh, T.S.G.A.M., Van Winkle, T., Cullen, J.M., Charles, J.A., Desmet, V.J., 2006. Morphological Classification of Parenchymal Disorders of the Canine and Feline Liver: 2. Hepatocellular Death, Hepatitis and Cirrhosis. In: WSAVA Liver Standardization, Rothuizen, J., Bunch, S.E., Charles, J.A., Cullen, J.M., Desmet, V.J., Szatmári, V., Twedt, D.C., van den Ingh, T.S.G.A.M., Van Winkle, T., Washabau, R.J. (Eds.), WSAVA Standards for Clinical and Histological Diagnosis of Canine and Feline Liver Diseases. W.B. Saunders, Edinburgh, pp. 85–101.
van der Zande, M., Vandebriel, R.J., Van Doren, E., Kramer, E., Herrera Rivera, Z., Serrano-Rojero, C.S., Gremmer, E.R., Mast, J., Peters, R.J., Hollman, P.C., Hendriksen, P.J., Marvin, H.J., Peijnenburg, A.A., Bouwmeester, H., 2012. Distribution, elimination, and toxicity of silver nanoparticles and silver ions in rats after 28-day oral exposure. ACS Nano 6, 7427–7442. https://doi.org/10.1021/nn302649p.
Walker, F., 1971. Experimental argyria: a model for basement membrane studies. Br. J. Exp. Pathol. 52, 589–593.
Walker, F., 1972. The deposition of silver in glomerular basement membrane. Virchows Arch. B Cell Pathol. 11, 90–96.
Walters, C.R., Pool, E.J., Somerset, V.S., 2014. Ecotoxicity of silver nanomaterials in the aquatic environment: a review of literature and gaps in nano-toxicological research. J Environ Sci Health A Tox Hazard Subst Environ Eng 49, 1588–1601. https://doi.org/10.1080/10934529.2014.938536.
Wang, H., Ho, K.T., Scheckel, K.G., Wu, F., Cantwell, M.G., Katz, D.R., Horowitz, D.B., Boothman, W.S., Burgess, R.M., 2014. Toxicity, bioaccumulation, and biotransformation of silver nanoparticles in marine organisms. Environ. Sci. Technol. 48, 13711–13717. https://doi.org/10.1021/es502976y.
Woshner, V.M., O'Hara, T.M., Bratton, G.R., Suydam, R.S., Beasley, V.R., 2001. Concentrations and interactions of selected essential and non-essential elements in bowhead and beluga whales of arctic Alaska. J. Wildl. Dis. 37, 693–710. https://doi.org/10.7589/0090-3558-37.4.693.
Yang, J., Miyazaki, N., 2003. Moisture content in Dall's porpoise (*Phocoenoides dalli*) tissues: a reference base for conversion factors between dry and wet weight trace element concentrations in cetaceans. Environ. Pollut. 121, 345–347. https://doi.org/10.1016/S0269-7491(02)00239-7.
Yoneda, S., Suzuki, K.T., 1997a. Detoxification of mercury by selenium by binding of equimolar Hg-Se complex to a specific plasma protein. Toxicol. Appl. Pharmacol. 143, 274–280. https://doi.org/10.1006/taap.1996.8095.
Yoneda, S., Suzuki, K.T., 1997b. Equimolar Hg-Se complex binds to selenoprotein P. Biochem. Biophys. Res. Commun. 231, 7–11. https://doi.org/10.1006/bbrc.1996.6036.
Yu, S.J., Yin, Y.G., Liu, J.F., 2013. Silver nanoparticles in the environment. Environ Sci Process Impacts 15, 78–92. https://doi.org/10.1039/C2EM30595J.
Zarnescu, O., Petrescu, A.M., Gaspar, A., Craciunescu, O., 2017. Effect of sublethal nickel chloride exposure on crayfish, *Astacus leptodactylus* ovary: an ultrastructural, autometallographic, and electrophoretic analyses. Microsc. Microanal. 23, 668–678. https://doi.org/10.1017/S1431927617000496.
Zhu, L., Tang, Y., Wang, H.D., Zhang, Z.Y., Pan, H., 2012. Immersion autometallographic demonstration of pathological zinc accumulation in human acute neural diseases. Neurol. Sci. 33, 855–861. https://doi.org/10.1007/s10072-011-0847-2.